ACS APPLIED MATERIALS & INTERFACES

Forum Article

www.acsami.org

A Microporous Amic Acid Polymer for Enhanced Ammonia Capture

Ji-Woong Lee,[†,‡,§,#] Gokhan Barin,[†,‡,#] Gregory W. Peterson,[∥] Jun Xu,[⊥] Kristen A. Colwell,[‡,⊥] and Jeffrey R. Long*[,†,‡,⊥]

[†]Department of Chemistry, University of California, Berkeley, California 94720, United States

[‡]Materials Sciences Division, Lawrence Berkeley National Laboratory, Berkeley, California 94720, United States

[§]Department of Chemistry, University of Copenhagen, 2100 Copenhagen, Denmark

[∥]Edgewood Chemical Biological Center, U.S. Army Research, Development, and Engineering Command, 5183 Blackhawk Road, Aberdeen Proving Ground, Maryland 21010, United States

[⊥]Department of Chemical and Biological Engineering, University of California, Berkeley, California 94720, United States

Supporting Information

ABSTRACT: Amic acids, consisting of carboxylic acids and amides, are often utilized as intermediates that can further undergo a dehydration−cyclization step to yield polymeric cyclic imides. Compared with imide-based materials, the presence of Brønsted acidic groups and multiple hydrogen-bond donors and acceptors in materials incorporating amic acids opens up the possibility for a variety of host−guest interactions. Here we report a facile and catalyst-free synthesis of a Brønsted acidic porous poly(amic acid) (PAA) and present its NH_3 uptake properties using gas adsorption and breakthrough measurements. Simple addition of water as a cosolvent to a mixture of tetrakis(4-aminophenyl)methane and pyromellitic anhydride resulted in the formation of PAA in almost quantitative yield. Further mechanistic studies with model compounds revealed the importance of additive water to generate amic acid species selectively without forming cyclic imides at high temperatures. Gas adsorption isotherms and breakthrough curves obtained under dry and humid conditions demonstrate the enhanced NH_3 uptake in the case of PAA compared with the related polycyclic imide at both low and high pressures. Furthermore, the results of adsorption/desorption cycling experiments provide insights into the strength of the interaction between ammonia and the polymers.

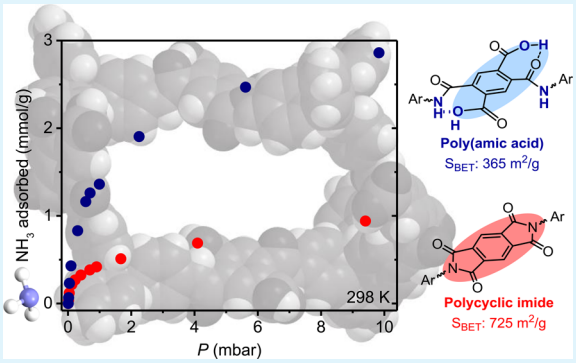

KEYWORDS: *porous polymers, gas capture, ammonia, poly(amic acid), polycyclic imide*

INTRODUCTION

The organization of hydrogen-bonding networks in three-dimensional space is of great interest for various fields of science, inspiring artificial construction of materials with tailored functionality and performance.[1] Although the strength of a single hydrogen bond is considered to be relatively weak (2−10 kcal/mol), their collective action and presence at a high density can induce striking differences in the overall structures and properties of materials.[2−5] Among many hydrogen-bond donors, amides present one of the most accessible and outstanding functional groups to donate and accept hydrogen bonds simultaneously,[6] as exemplified by their utilization in high-tensile-strength synthetic polymers such as nylon and aramid fibers.[7] The macroscopic strength of these polymers is attributed to the presence of infinite hydrogen-bonding networks of amides (C═O···H−N; Figure 1) and in part to aromatic $\pi-\pi$ stacking in the case of aramids. As such, the ability to control structural organization rationally in these types of materials is crucial in order to tailor their functionality for a desired application.[8]

Despite the abundance of amide bonds in biological and artificial materials, the application and manipulation of amide bonds at macroscopic scales can be challenging because of intramolecular and intermolecular amide−amide interactions that sometimes significantly hinder the desired host−guest interactions in high-molecular-weight coordination polymers.[9] Amic acids, on the other hand, can in principle provide multiple available interaction sites because of the proximal flexible hydrogen-bond donors and acceptors (i.e., an amide and a carboxylic acid). However, poly(amic acids) have been intensively studied mainly as an intermediate to access polycyclic imides,[10−12] and their application as acid-functionalized polymers, particularly in a porous environment, has not been realized to date.

Special Issue: Hupp 60th Birthday Forum

Received: February 22, 2017
Accepted: March 31, 2017

DOI: 10.1021/acsami.7b02603
ACS Appl. Mater. Interfaces XXXX, XXX, XXX−XXX

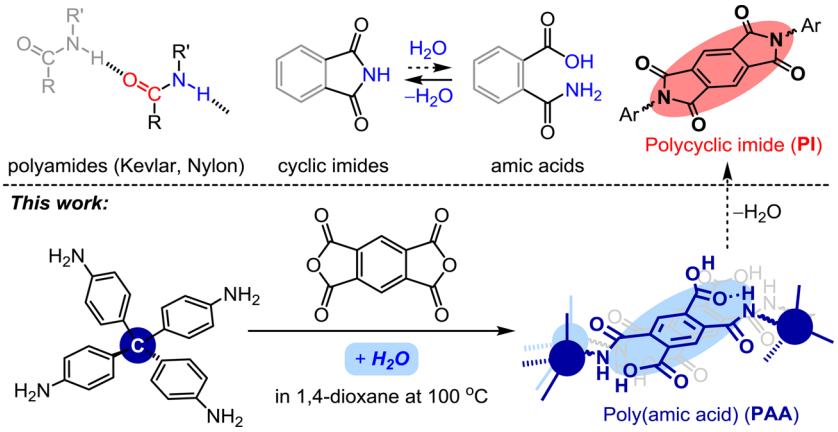

Figure 1. (top) Structures of polyamides, cyclic imides, amic acids, and polycyclic imides. (bottom) The synthesis of PAA was achieved using tetrakis(4-aminophenyl)methane and pyromellitic anhydride in a water/1,4-dioxane mixture. PI was prepared using the same monomers in the absence of water.

Solid-state materials with permanent porosity, such as metal−organic frameworks,[13−18] covalent organic frameworks,[19−23] and porous polymers,[24−30] have received significant attention, especially for gas separation, storage, and capture applications. An important advantage of these materials over traditional porous materials is the high degree of structural and functional control in their preparation for a specific application. In particular, porous polymers offer significant advantages due to (i) their high stability, originating from their covalent nature, and (ii) the level of synthetic control, which allows the incorporation of various functional groups (e.g., Brønsted acids or bases) that would otherwise interfere in the cases of metal−organic frameworks and covalent organic frameworks. To this end, our laboratory has recently demonstrated that framework interpenetration in a Brønsted acid-funtionalized porous polymer increases the proximity of functional groups within the pores, which led to enhanced host−guest interactions and was shown to enable the highly effective capture of ammonia, even at low concentrations.[31] The development of new solid-state adsorbents for the efficient capture of ammonia from air (or, more broadly, hazardous gas capture) is of great importance because of the toxicity and volatility of ammonia as well as its widespread utilization in various sectors of industry.[32] In a previous study, we particularly showed that a carboxylic acid-decorated porous polymer with an interpenetrated structure displays significantly enhanced NH_3 uptake capacity compared with a non-interpenetrated polymer incorporating sulfonic acids, despite the weaker acidity of the former.[31] This result was attributed to the cooperative action of multiple carboxylic acid groups by means of Brønsted acidity and hydrogen-bonding interactions due to the increased proximity of functional groups in an interpenetrated structure, leading to stronger overall acidity. It is important to note that the preparation of these polymers typically requires multiple synthetic steps and involves metal-catalyzed coupling reactions.

We therefore sought a facile synthetic methodology that can afford porous polymers with a high density of Brønsted acid groups and hydrogen-bond donors and acceptors to remove ammonia efficiently. A porous poly(amic acid) could serve as an ideal platform to achieve this goal because of (i) the stability of amide bonds, creating a robust framework; (ii) its hydrophilicity, which could potentially enhance its NH_3 uptake under humid conditions; and (iii) intramolecular and intermolecular hydrogen-bonding interactions within the poly(amic acid) that could strengthen the acidity of carboxylic acids or amides (see Figure S1 for a comparison of calculated acidities of carboxylic acid, amide, and amic acid). Polyimides with intrinsic microporosity have recently been synthesized and investigated for a number of gas storage and separation applications.[33−37] In view of the chemical stability of cyclic imides, the installation of Brønsted acidic groups via partial hydrolysis of imides to amic acids could be cumbersome.[10] Thus, we envisioned that the direct synthesis of poly(amic acids) while generating a porous network is practically more relevant.

Herein we report a facile and catalyst-free one-step approach to obtaining a Brønsted acidic porous poly(amic acid) (PAA) from simple starting materials, including tetrakis(4-aminophenyl)methane and pyromellitic anhydride (Figure 1), and describe its ammonia removal performance under dry and humid conditions. Because of the presence of amic acid functionality, PAA possesses a high density of Brønsted acidic sites (−CO_2H, theoretically 4.9 mmol/g) and is also enriched with additional hydrogen-bond donors (−CONH−, theoretically 4.9 mmol/g) and acceptors (C═O, 9.8 mmol/g). Furthermore, the highly accessible nature of these functional sites in a porous environment renders this material a promising platform for the effective capture of ammonia at the low pressures that are relevant to its removal from air. Control experiments with model compounds and a related porous polycyclic imide (PI) confirm the structural features of PAA and the advantages of the amic acid functionality for the capture of ammonia.

RESULTS AND DISCUSSION

In order to access PAA, we presumed that the presence of water would interrupt the formation of PI by suppressing the dehydration−cyclization step following the initial amide formation.[10] PAA was therefore synthesized upon reacting tetrakis(4-aminophenyl)methane and pyromellitic anhydride in a water/organic solvent mixture at 100 °C.[38] After screening of multiple reaction conditions (Table S1), a water/1,4-dioxane mixture (5% water, v/v) was determined to be the best solvent mixture to access PAA in high yields (>95%) while maintaining its porosity. The effect of water, as well as its ratio, in the reaction medium to obtain PAA was initially monitored by Fourier transform infrared (FT-IR) spectroscopy (Figure 2A). In the absence of water, we observed essentially no amide C═

DOI: 10.1021/acsami.7b02603
ACS Appl. Mater. Interfaces XXXX, XXX, XXX−XXX

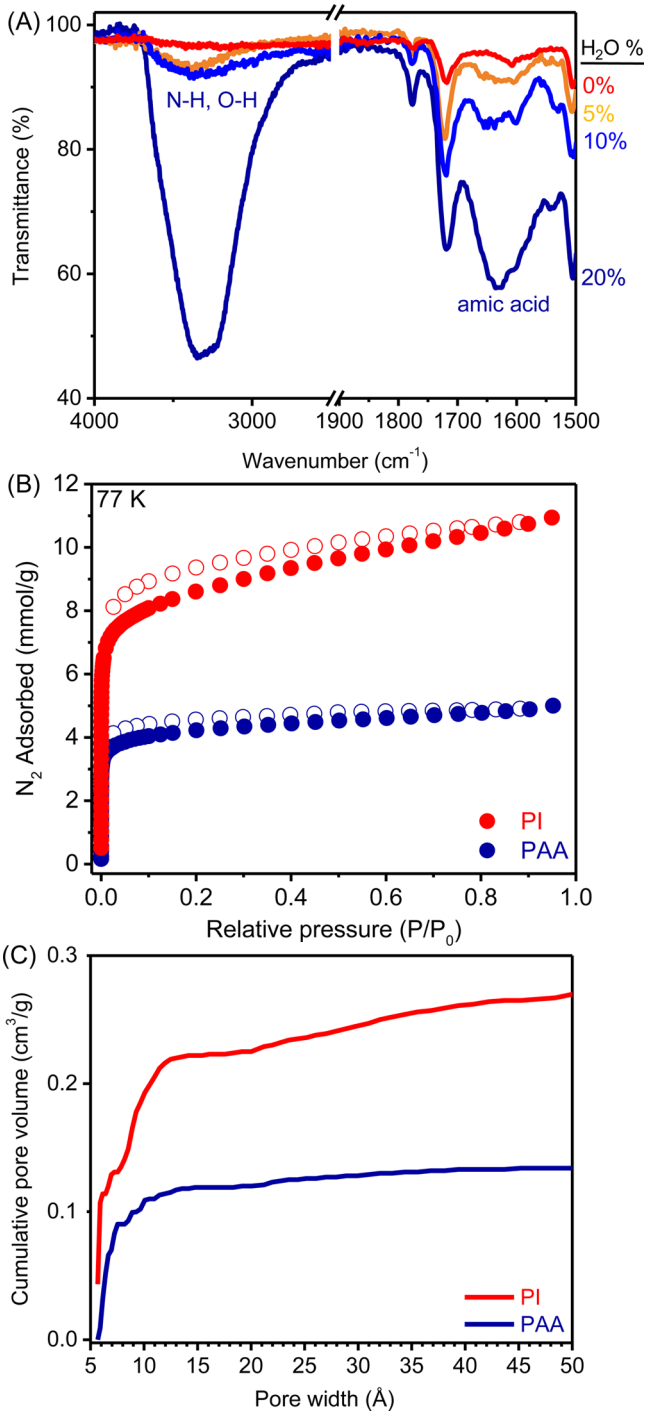

Figure 2. (A) FT-IR spectra of polymerization products upon changing the amount of water in 1,4-dioxane. (B) Nitrogen isotherms of PI and PAA at 77 K. Solid and open symbols represent the adsorption and desorption branches, respectively. (C) Pore size distributions of PI and PAA.

O stretching band at 1630 cm^{-1} associated with the formation of amic acid species (Figure 2A, red line). A water content of up to 20% (v/v) in 1,4-dioxane was tolerated for the formation of PAA at the expense of low reaction yields (Table S1). It should be noted that the presence of a C═O stretching band at 1718 cm^{-1} in the FT-IR spectra while using water as a cosolvent indicates that imide formation still occurs to some extent in the resulting PAA samples. In order to compare with PAA, a high-surface area sample of PI was also prepared using a previously reported procedure.[37,39,40] Notably, in comparison with that of PI, the FT-IR spectrum of PAA after drying under vacuum at 80 °C exhibits a strong absorption band associated with N−H and O−H stretching vibrations (Figure S5).

Surface area and porosity analyses were carried out using N_2 gas adsorption isotherms collected at 77 K. Both PAA and PI display reversible type-I isotherms, indicating their microporous nature (Figure 2B). The Brunauer−Emmett−Teller (BET) surface areas of PAA and PI were found to be 365 and 725 m^2/g, respectively. Interestingly, pore size analysis (Figure 2C) shows that PAA is composed of pores mostly located in the 5−6 Å region, whereas in the case of PI there is an additional significant pore volume contribution from the pores centered around ∼9 Å. Scanning electron microscopy (SEM) images demonstrate that both PAA and PI have spherical particles with sizes in the range of 100−500 nm (Figure S6). Thermogravimetric analysis (TGA) further provides evidence for the presence of amic acid groups within PAA (Figure S9). This polymer displays an initial weight loss up to 100 °C, which can be attributed to the removal of solvent molecules from the pores, and a second loss in the 100−200 °C region due to the loss of water molecules associated with the cyclic imidization reaction of amic acids. This second weight loss step is absent in the TGA trace of PI, supporting imidization of PAA upon thermal treatment. The observed weight loss during the imidization process (based on the mass of the dry sample after initial solvent loss) corresponds to 7.9%, which is close to the theoretical value of 8.8% calculated for the imidization of an ideal PAA structure. Furthermore, we performed another TGA experiment in which a PAA sample was kept at 250 °C for 90 min in order to ensure complete imidization (Figure S10). The structural changes were monitored by FT-IR spectroscopy, confirming that the amide C═O stretching band of the amic acid at 1630 cm^{-1} in PAA disappears from the spectrum after thermal treatment (Figure S11). These results verify the formation of amic acid functionality in PAA using our synthetic approach.

To gain further structural insights into PAA, we performed model compound studies using monofunctional analogues of tetrakis(4-aminophenyl)methane and pyromellitic anhydride (Scheme 1). First, tetrakis(4-aminophenyl)methane was reacted with 4 equiv of phthalic anhydride under the same reaction conditions used for the preparation of PAA (water/1,4-dioxane, 100 °C, 18 h). Following evaporation of the reaction solvents, the crude reaction mixture was subjected to elemental analysis, mass spectrometry, and NMR spectroscopy. High-resolution mass spectrometry and elemental analysis data unambiguously show the formation of MC-1, which is a fourfold amic acid product, as a major product (Scheme 1A). Although many rotational isomers can potentially exist in the solution state as a result of the amide bonds, the ^1H and ^{13}C NMR spectra of the crude MC-1 product exhibit one set of signals in DMSO-d_6 without any indication of cyclic imide formation (Figure S2). While further analysis is required, this preliminary result indicates the advantage of the tetrahedral building unit (tetrakis(4-aminophenyl)methane), for which the four functional groups react largely independently.

Additional model compound studies were performed using aniline and pyromellitic anhydride, which gave rise to two regioisomers (MC-2A and MC-2B) and their corresponding rotamers (Scheme 1B). On the basis of high-resolution mass spectrometry and elemental analysis, the crude reaction product

DOI: 10.1021/acsami.7b02603
ACS Appl. Mater. Interfaces XXXX, XXX, XXX−XXX

Scheme 1. Synthesis of Model Compounds (A) MC-1 and (B) MC-2 and the Corresponding Characterization Data from High-Resolution Mass Spectroscopy and Elemental Analysis; Shown in the Boxes Are Compounds That Could Potentially Form via Imidization of MC-1 and MC-2

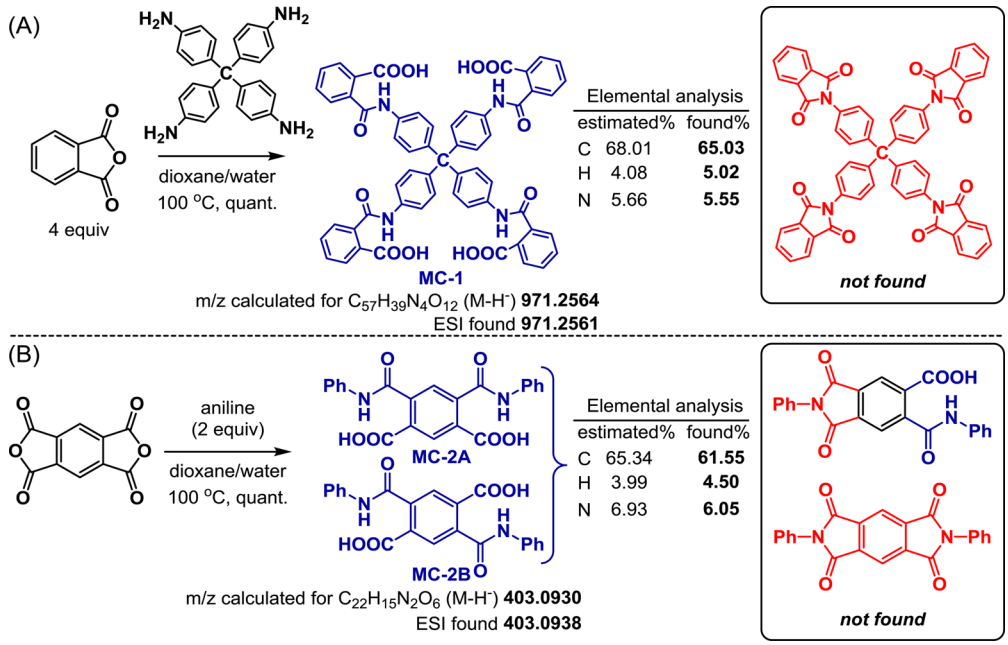

was found to be free of mono- and bicyclic imide. Accordingly, the ^{13}C NMR spectrum of the crude product was tentatively assigned as a mixture of MC-2A and MC-2B, and clear interpretation of the crude NMR spectra was not feasible because of the complexity of the amide rotamers (Figure S3). Nonetheless, these model studies strongly suggest the advantage of having water present in the reaction medium, such that the chemical equilibrium can be manipulated to generate the amic acid functionality (and therefore PAA) selectively while preventing the formation of cyclic imide via further dehydration.

Next, the ammonia uptakes by PAA and PI were investigated at pressures of up to 1 bar at 298 K under dry conditions (Figure 3A). The comparison of these two adsorption isotherms is important in order to understand the influence of Brønsted acidic sites and multiple hydrogen-bond donors and acceptors within PAA. First of all, PAA demonstrates a steeper uptake behavior in the low-pressure region compared with PI while also displaying a greater ammonia loading capacity (Figure 3A, B). While PAA has an uptake capacity of 10.7 mmol/g at 1 bar, PI exhibits a slightly lower adsorption capacity of 9.0 mmol/g at the same pressure. Despite the fact that PAA has a lower surface area than PI, the presence of Brønsted acidic and hydrogen-bonding sites likely accounts for the overall enhanced performance of PAA. More interestingly, PAA also demonstrates significantly higher ammonia uptake than PI at pressures as low as 1 mbar, which is relevant to ammonia removal from air. The uptake capacity of PAA at 1 mbar was estimated to be 1.6 mmol/g, whereas a capacity of 0.4 mmol/g was obtained for PI (Figure 3B). The uptake capacity of PI reaches only ~1 mmol/g at 10 mbar, emphasizing the positive effect of Brønsted acidic groups and additional hydrogen-bond donor sites for the enhanced performance in the case of PAA.

To further investigate the strength of ammonia interaction and assess the recyclability of both PAA and PI, we carried out adsorption/desorption cycling experiments at 25 °C with an equilibrium NH_3 pressure of 1 mbar. Samples were reactivated between successive cycles under vacuum at room temperature (25 °C) or 80 °C, as specified in Figure 3C. After the first cycle of adsorption, regeneration at room temperature did not fully recover the initial capacities, as observed from the uptake amounts observed in the second and third cycles, indicating that some portion of ammonia was retained strongly by both PAA and PI. However, upon heating at 80 °C for 4 h (fourth cycle), 87% of the initial ammonia capacity was restored for PI, whereas PAA exhibited only 65% of the capacity obtained in the first cycle. Prolonged heating at 80 °C (18 h, fifth cycle) did not change the NH_3 uptake of PI significantly, but that of PAA was further improved. This behavior can be attributed to the presence of strong interactions with Brønsted acidic sites in PAA. We also investigated the adsorption kinetics of ammonia in the low-pressure region (up to 3 mbar). At an equilibrium pressure of 0.3 mbar, PAA almost reached equilibrium within 1 min, while lower adsorption rates were observed as the pressure was increased progressively (Figure S12). Such a decrease in rate can be explained by the accumulation of NH_3 molecules within the pores, such that the diffusion of additional gas molecules introduced at higher pressures becomes slower, causing the system to take a longer to reach equilibrium. A comparison of the kinetic uptake curves for PAA and PI at 3 mbar shows that PI reaches equilibrium faster than PAA, most likely because of its larger pore volume and higher surface area, which facilitate the diffusion of NH_3 molecules (Figure S13).

Lastly, the performance of PAA and PI for the removal of ammonia was investigated under practical conditions[41−43] using dynamic microbreakthrough measurements at 293 K. The experiments were performed under dry as well as humid (80% relative humidity (RH)) conditions to study the effect of water, which is typically detrimental to uptake capacities for materials with Lewis acidic sites.[44−46] The partial pressure of ammonia in the feed stream (2000 mg/m^3) was approximately 2.8 mbar.

DOI: 10.1021/acsami.7b02603
ACS Appl. Mater. Interfaces XXXX, XXX, XXX−XXX

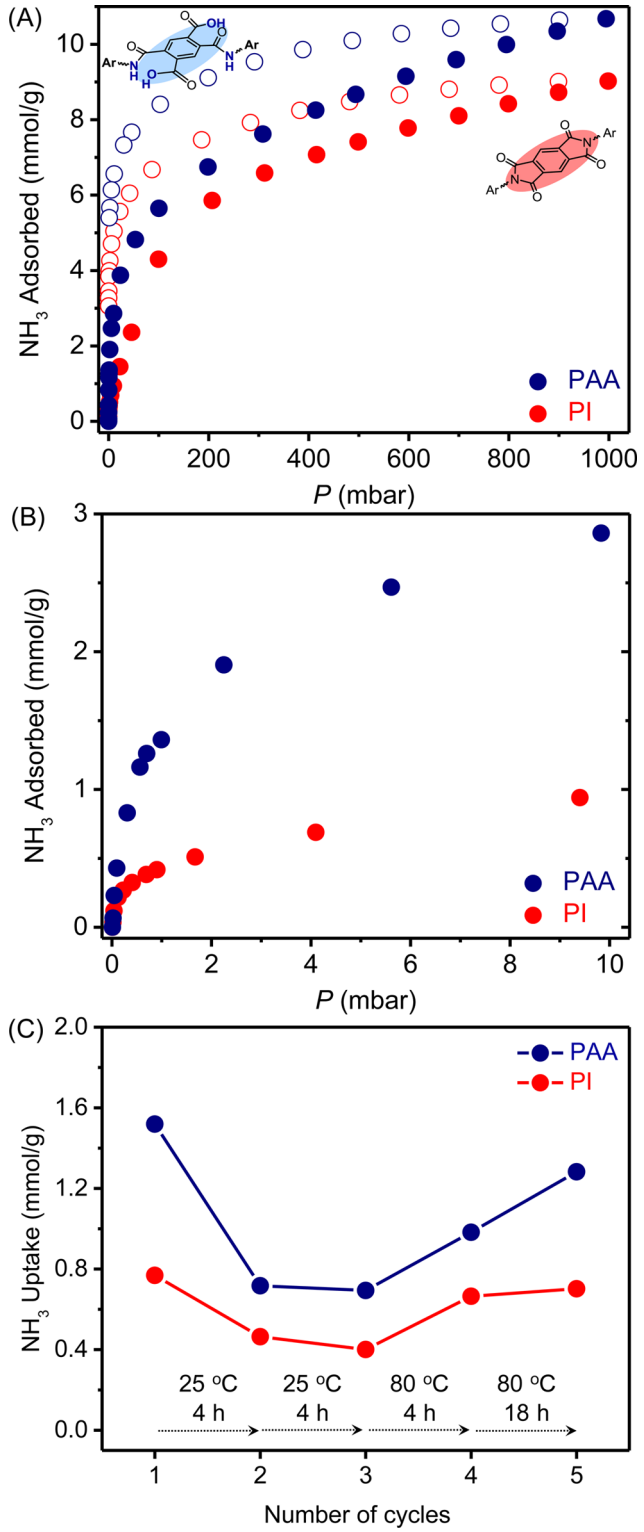

Figure 3. (A) NH_3 adsorption isotherms of PI and PAA at 298 K. Solid and open symbols represent the adsorption and desorption branches, respectively. (B) Low-pressure region (0−10 mbar) of NH_3 isotherms. (C) Cycling adsorption/desorption experiments at an equilibrium NH_3 pressure of 1 mbar. Regeneration conditions between successive cycles are specified on the plot.

Both materials exhibit steep breakthrough curves, indicating that the uptake process is not diffusion-controlled (Figure 4). Under dry conditions, PI displays a saturation uptake capacity of 1.1 mmol/g, which is lower than that of PAA (2.4 mmol/g).

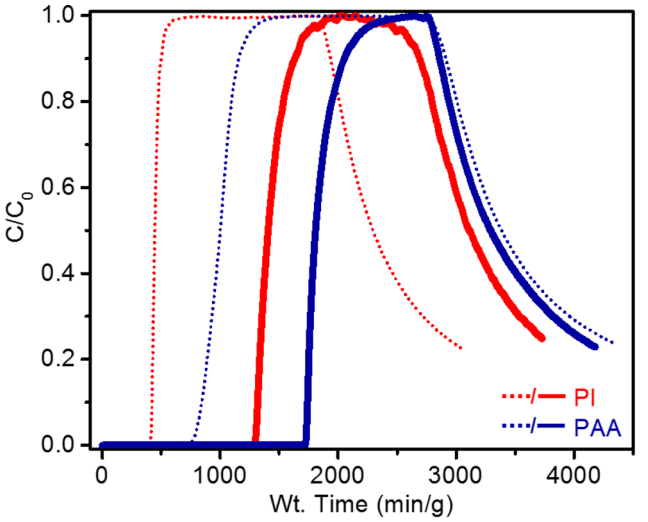

Polymer	Saturation NH_3 loadings (mmol/g)	
	Dry (0% RH)	Humid (80% RH)
PI	1.1	3.4
PAA	2.4	4.4

Figure 4. Breakthrough curves for PI and PAA under dry (dashed lines) and humid (80% RH; solid lines) conditions. After saturation, desorption curves were obtained upon purging the column with dry or humid air. The table summarizes the NH_3 saturation capacities of PI and PAA.

Notably, these values are in agreement with those obtained from gas adsorption measurements. In the presence of humidity, both PI and PAA exhibit enhanced saturation capacities of 3.4 and 4.4 mmol/g, respectively.[47] A positive effect of water on the uptake capacity has also been demonstrated for other materials.[48] In the case of PAA, it is likely that the interaction between ammonia and multiple polar surface groups originating from the amic acid functionality is enhanced in the presence of water by means of the creation of an extended hydrogen-bonding network.[32] In addition, water molecules could facilitate the proton transfer from carboxylic acids to ammonia to form ammonium cations.[49] It is important to note that the saturation capacity of PI under humid conditions corresponds to more than 3 times its dry capacity, whereas the overall improvement in the case of PAA is slightly less than twice its dry uptake. Dissolution of ammonia potentially plays an important role in NH_3 capture under humid conditions and is observed to be more pronounced in the case of PI because of its larger surface area and pore volume, which can accommodate more water molecules.

CONCLUSIONS

We have developed a simple synthetic strategy for the preparation of a porous poly(amic acid) (PAA) and demonstrated its efficacy in the capture of ammonia from air. The key to access the amic acid-functionalized polymer while maintaining the porous nature of the resulting material is the utilization of water as a cosolvent (5% in 1,4-dioxane) at high temperatures, which suppresses the further formation of imides from amic acid via a dehydration−cyclization step. The high density of Brønsted acidic ($-CO_2H$) groups and hydrogen-bonding sites, their accessibility in a porous environment, and high chemical and thermal stabilities render PAA a promising material for NH_3 capture applications. Adsorption isotherms

DOI: 10.1021/acsami.7b02603
ACS Appl. Mater. Interfaces XXXX, XXX, XXX−XXX

and breakthrough curves obtained under dry and humid conditions for PAA, as well as for the related porous polycyclic imide PI, demonstrate the enhanced NH_3 removal performance at both low and high pressures due to the presence of amic acid functionality. Further investigations of the role of amide functional groups will be critical to improve the capacity and performance of porous poly(amic acid)s. The facile and potentially low-cost synthesis of PAA from simple reactants under catalyst-free reaction conditions is particularly attractive for its utility in personal protection equipment and air filtration applications.

■ ASSOCIATED CONTENT

Supporting Information

The Supporting Information is available free of charge on the ACS Publications website at DOI: 10.1021/acsami.7b02603.

Experimental details, including synthesis and characterization of PAA and PI; ^1H and ^{13}C NMR spectra of model compounds; TGA experiments; and NH_3 uptake kinetics data (PDF)

■ AUTHOR INFORMATION

Corresponding Author

*E-mail: jrlong@berkeley.edu.

ORCID

Ji-Woong Lee: 0000-0001-6177-4569

Author Contributions

#J.-W.L. and G.B. contributed equally.

Notes

The authors declare no competing financial interest.

■ ACKNOWLEDGMENTS

The collection and interpretation of solid-state NMR spectra and ammonia adsorption data were supported through the Center for Gas Separations Relevant to Clean Energy Technologies, an Energy Frontier Research Center funded by the U.S. Department of Energy, Office of Science, Office of Basic Energy Sciences, under Award DE-SC0001015. All other aspects of this research, including the synthesis of the new porous polymers, were supported by the Laboratory Directed Research and Development Program of Lawrence Berkeley National Laboratory under U.S. Department of Energy Contract DE-AC02-05CH11231. We thank the Miller Institute for Basic Research in Science for support of G.B. with a postdoctoral fellowship. We also thank Dr. Zachary P. Smith for helpful discussions.

■ REFERENCES

(1) van Kuringen, H. P. C.; Schenning, A. P. H. J. Hydrogen Bonding in Supramolecular Nanoporous Materials. In *Hydrogen Bonded Supramolecular Materials*; Li, Z.-T., Wu, L.-Z., Eds.; Springer: Berlin, 2015; pp 43−67.

(2) Martin, T. W.; Derewenda, Z. S. The Name is Bond - H bond. *Nat. Struct. Biol.* **1999**, *6*, 403−406.

(3) Paleos, C. M.; Tsiourvas, D. Molecular Recognition of Organized Assemblies via hydrogen bonding in aqueous media. *Adv. Mater.* **1997**, *9*, 695−710.

(4) Lemieux, R. U. How Water Provides the Impetus for Molecular Recognition in Aqueous Solution. *Acc. Chem. Res.* **1996**, *29*, 373−380.

(5) MacGillivray, L. R.; Atwood, J. L. A Chiral Spherical Molecular Assembly Held Together by 60 Hydrogen Bonds. *Nature* **1997**, *389*, 469.

(6) Johansson, A.; Kollman, P.; Rothenberg, S.; McKelvey, J. Hydrogen Bonding Ability of the Amide Group. *J. Am. Chem. Soc.* **1974**, *96*, 3794−3800.

(7) Marchildon, K. Polyamides − Still Strong After Seventy Years. *Macromol. React. Eng.* **2011**, *5*, 22−54.

(8) Lee, J.-W.; Mayer-Gall, T.; Opwis, K.; Song, C. E.; Gutmann, J. S.; List, B. Organotextile Catalysis. *Science* **2013**, *341*, 1225−1229.

(9) Hasegawa, S.; Horike, S.; Matsuda, R.; Furukawa, S.; Mochizuki, K.; Kinoshita, Y.; Kitagawa, S. Three-Dimensional Porous Coordination Polymer Functionalized with Amide Groups Based on Tridentate Ligand: Selective Sorption and Catalysis. *J. Am. Chem. Soc.* **2007**, *129*, 2607−2614.

(10) Sroog, C. E. Polyimides. *Prog. Polym. Sci.* **1991**, *16*, 561−694.

(11) Yu, J. W.; Choi, Y.-M.; Jung, J.; You, N.-H.; Lee, D. S.; Lee, J.-K.; Goh, M. Highly Microporous Carbon Materials Synthesized from Fluorine-Containing Poly(Amic Acid) Adsorbed in Polystyrene Cryogel Template. *Synth. Met.* **2016**, *211*, 35−39.

(12) Kim, S.; Jang, K.-S.; Choi, H.-D.; Choi, S.-H.; Kwon, S.-J.; Kim, I.-D.; Lim, J.; Hong, J.-M. Porous Polyimide Membranes Prepared by Wet Phase Inversion for Use in Low Dielectric Applications. *Int. J. Mol. Sci.* **2013**, *14*, 8698−8707.

(13) Ferey, G. Hybrid Porous Solids: Past, Present, Future. *Chem. Soc. Rev.* **2008**, *37*, 191−214.

(14) Horike, S.; Shimomura, S.; Kitagawa, S. Soft Porous Crystals. *Nat. Chem.* **2009**, *1*, 695−704.

(15) O'Keeffe, M.; Yaghi, O. M. Deconstructing the Crystal Structures of Metal−Organic Frameworks and Related Materials into Their Underlying Nets. *Chem. Rev.* **2012**, *112*, 675−702.

(16) Zhou, H.-C.; Long, J. R.; Yaghi, O. M. Introduction to Metal−Organic Frameworks. *Chem. Rev.* **2012**, *112*, 673−674.

(17) Furukawa, H.; Cordova, K. E.; O'Keeffe, M.; Yaghi, O. M. The Chemistry and Applications of Metal-Organic Frameworks. *Science* **2013**, *341*, 1230444.

(18) Zhou, H. C.; Kitagawa, S. Metal-Organic Frameworks (MOFs). *Chem. Soc. Rev.* **2014**, *43*, 5415−5418.

(19) Waller, P. J.; Gándara, F.; Yaghi, O. M. Chemistry of Covalent Organic Frameworks. *Acc. Chem. Res.* **2015**, *48*, 3053−3063.

(20) Feng, X.; Ding, X.; Jiang, D. Covalent Organic Frameworks. *Chem. Soc. Rev.* **2012**, *41*, 6010−6022.

(21) Ding, S.-Y.; Wang, W. Covalent Organic Frameworks (COFs): from Design to Applications. *Chem. Soc. Rev.* **2013**, *42*, 548−568.

(22) Colson, J. W.; Dichtel, W. R. Rationally Synthesized Two-Dimensional Polymers. *Nat. Chem.* **2013**, *5*, 453−465.

(23) Slater, A. G.; Cooper, A. I. Function-Led Design of New Porous Materials. *Science* **2015**, *348*, aaa8075.

(24) McKeown, N. B.; Budd, P. M. Polymers of Intrinsic Microporosity (PIMs): Organic Materials for Membrane Separations, Heterogeneous Catalysis and Hydrogen Storage. *Chem. Soc. Rev.* **2006**, *35*, 675−683.

(25) Thomas, A. Functional Materials: From Hard to Soft Porous Frameworks. *Angew. Chem., Int. Ed.* **2010**, *49*, 8328−8344.

(26) Kaur, P.; Hupp, J. T.; Nguyen, S. T. Porous Organic Polymers in Catalysis: Opportunities and Challenges. *ACS Catal.* **2011**, *1*, 819−835.

(27) Dawson, R.; Cooper, A. I.; Adams, D. J. Nanoporous Organic Polymer Networks. *Prog. Polym. Sci.* **2012**, *37*, 530−563.

(28) Zhang, Y.; Riduan, S. N. Functional Porous Organic Polymers for Heterogeneous Catalysis. *Chem. Soc. Rev.* **2012**, *41*, 2083−2094.

(29) Wu, D.; Xu, F.; Sun, B.; Fu, R.; He, H.; Matyjaszewski, K. Design and Preparation of Porous Polymers. *Chem. Rev.* **2012**, *112*, 3959−4015.

(30) Muller, T.; Brase, S. Tetrahedral Organic Molecules as Components in Supramolecular Architectures and in Covalent Assemblies, Networks and Polymers. *RSC Adv.* **2014**, *4*, 6886−6907.

(31) Van Humbeck, J. F.; McDonald, T. M.; Jing, X.; Wiers, B. M.; Zhu, G.; Long, J. R. Ammonia Capture in Porous Organic Polymers Densely Functionalized with Brønsted Acid Groups. *J. Am. Chem. Soc.* **2014**, *136*, 2432−2440.

DOI: 10.1021/acsami.7b02603
ACS Appl. Mater. Interfaces XXXX, XXX, XXX−XXX

(32) DeCoste, J. B.; Peterson, G. W. Metal−Organic Frameworks for Air Purification of Toxic Chemicals. *Chem. Rev.* **2014**, *114*, 5695−5727.
(33) Peterson, G. W.; Farha, O. K.; Schindler, B.; Jones, P.; Mahle, J.; Hupp, J. T. Evaluation of a Robust, Diimide-Based, Porous Organic Polymer (POP) as a High-Capacity Sorbent for Representative Chemical Threats. *J. Porous Mater.* **2012**, *19*, 261−266.
(34) Li, G.; Wang, Z. Microporous Polyimides with Uniform Pores for Adsorption and Separation of CO_2 Gas and Organic Vapors. *Macromolecules* **2013**, *46*, 3058−3066.
(35) Fang, Q.; Wang, J.; Gu, S.; Kaspar, R. B.; Zhuang, Z.; Zheng, J.; Guo, H.; Qiu, S.; Yan, Y. 3D Porous Crystalline Polyimide Covalent Organic Frameworks for Drug Delivery. *J. Am. Chem. Soc.* **2015**, *137*, 8352−8355.
(36) Weber, J.; Su, Q.; Antonietti, M.; Thomas, A. Exploring Polymers of Intrinsic Microporosity − Microporous, Soluble Polyamide and Polyimide. *Macromol. Rapid Commun.* **2007**, *28*, 1871−1876.
(37) Wang, Z.; Zhang, B.; Yu, H.; Sun, L.; Jiao, C.; Liu, W. Microporous Polyimide Networks with Large Surface Areas and Their Hydrogen Storage Properties. *Chem. Commun.* **2010**, *46*, 7730−7732.
(38) It should be noted that even though our attempts to synthesize PAA at room temperature (at which the synthesis of poly(amic acids) is performed before imidization) generated a precipitate, it was proven to be a nonporous material.
(39) Farha, O. K.; Spokoyny, A. M.; Hauser, B. G.; Bae, Y.-S.; Brown, S. E.; Snurr, R. Q.; Mirkin, C. A.; Hupp, J. T. Synthesis, Properties, and Gas Separation Studies of a Robust Diimide-Based Microporous Organic Polymer. *Chem. Mater.* **2009**, *21*, 3033−3035.
(40) Farha, O. K.; Bae, Y.-S.; Hauser, B. G.; Spokoyny, A. M.; Snurr, R. Q.; Mirkin, C. A.; Hupp, J. T. Chemical Reduction of a Diimide Based Porous Polymer for Selective Uptake of Carbon Dioxide versus Methane. *Chem. Commun.* **2010**, *46*, 1056−1058.
(41) Cal/OHSA Permissible Exposure Limits for Chemical Contaminants. http://www.dir.ca.gov/title8/5155table_ac1.html (accessed Jan 4, 2017).
(42) MacDonald, S. A.; Hinsberg, W. D.; Wendt, H. R.; Clecak, N. J.; Willson, C. G.; Snyder, C. D. Airborne Contamination of a Chemically Amplified Resist. 1. Identification of Problem. *Chem. Mater.* **1993**, *5*, 348−356.
(43) Lin, I-K.; Bai, H.; Wu, B.-J. Analysis of Relationship between Inorganic Gases and Fine Particles in Cleanroom Environment. *Aerosol Air Qual. Res.* **2010**, *10*, 245.
(44) DeCoste, J. B.; Denny, M. S., Jr.; Peterson, G. W.; Mahle, J. J.; Cohen, S. M. Enhanced Aging Properties of HKUST-1 in Hydrophobic Mixed-Matrix Membranes for Ammonia Adsorption. *Chem. Sci.* **2016**, *7*, 2711−2716.
(45) Peterson, G. W.; Wagner, G. W.; Balboa, A.; Mahle, J.; Sewell, T.; Karwacki, C. J. Ammonia Vapor Removal by $Cu_3(BTC)_2$ and Its Characterization by MAS NMR. *J. Phys. Chem. C* **2009**, *113*, 13906−13917.
(46) Takahashi, A.; Tanaka, H.; Parajuli, D.; Nakamura, T.; Minami, K.; Sugiyama, Y.; Hakuta, Y.; Ohkoshi, S.-i.; Kawamoto, T. Historical Pigment Exhibiting Ammonia Gas Capture beyond Standard Adsorbents with Adsorption Sites of Two Kinds. *J. Am. Chem. Soc.* **2016**, *138*, 6376−6379.
(47) To compare the NH_3 saturation uptake capacities of PAA and PI with commercially available porous carbon materials (up to 0.69 and 0.45 mmol/g, dry and humid conditions, respectively), see ref 33 and: Glover, T. G.; Peterson, G. W.; Schindler, B. J.; Britt, D.; Yaghi, O. MOF-74 Building Unit has a Direct Impact on Toxic Gas Adsorption. *Chem. Eng. Sci.* **2011**, *66*, 163−170.
(48) Huggins, M. L. Hydrogen Bridges in Organic Compounds. *J. Org. Chem.* **1936**, *1*, 407−456.
(49) Seredych, M.; Bandosz, T. J. Combined Role of Water and Surface Chemistry in Reactive Adsorption of Ammonia on Graphite Oxides. *Langmuir* **2010**, *26*, 5491−5498.

DOI: 10.1021/acsami.7b02603
ACS Appl. Mater. Interfaces XXXX, XXX, XXX−XXX